# Dielectric properties of dipicrylamine-doped erythrocytes, cultured cells and lipid vesicles

Koji Asami*

Institute for Chemical Research, Kyoto University, Uji, Kyoto 611-0011, Japan

* Tel: +81-774-38-3081, fax: +81-774-38-3084.
E-mail address: asami@e.kuicr.kyoto-u.ac.jp,

**Abstract**

Horse erythrocytes, murine lymphoblasts (L5178Y ) and lipid vesicles that were treated with dipicrylamine (DPA) as a lipophilic ion were studied by dielectric spectroscopy over a frequency range of 10 Hz to 10 MHz. The DPA-treated cells and lipid vesicles showed low-frequency (LF) dielectric dispersion around 1-10 kHz in addition to β-dispersion due to the Maxwell-Wagner effect. The LF dispersion corresponds to that found in previous electrorotation (ROT) studies on DPA-treated cells, being due to the translocation of mobile ions in the plasma membranes. Analysis of the LF dispersion based on the mobile charge model provided the area-specific concentration $N_t$ of DPA ions adsorbed at the membrane interfaces and their translocation rate constant $k_i$ between the interfaces. The values of $N_t$ and $k_i$ were respectively 13-21 nmol/m$^2$ and 0.7-1.6×10$^4$ s$^{-1}$ for both horse erythrocytes and L5178Y cells at 10 μM DPA, being consistent with those determined by ROT for human erythrocytes and cultured cells.

Keywords: Dielectric spectroscopy; Lipophilic ion; Mobile charge; Membrane; Erythrocyte.

## 1. Introduction

Effects of lipophilic ions such as tetraphenylborate and dipicrylamine (DPA) on the electric properties of planar bilayer lipid membranes (BLMs) were extensively studied in the early stage of planar BLM research [1-5]. The conductance and capacitance of BLMs were increased by the lipophilic ions, and the dynamic electric properties obtained by charge-pulse experiments showed fast and slow relaxation processes that correspond to charging of the "geometric" membrane and to translocation of mobile ions in the membranes, respectively. The slow relaxation was alternatively measured as low-frequency (LF) dielectric dispersion by impedance (or dielectric) spectroscopy [6].

The slow relaxation process was also found for the DPA-doped squid giant axon membranes by charge-pulse experiments using the internal electrode method [7]. For small cells, to which the internal electrode method is not applicable, the effects of lipophilic ions were studied by the electrorotation (ROT) method that measures the rotation speed of individual cells in rotating electric fields under an optical microscope. The rotation speed is a function of the imaginary part of the effective polarizability of the cell, depending on the frequency of the applied ac field. Using ROT, the LF dispersion due to lipophilic ions was found for erythrocytes [8] and cultured cells [9]. Zimmermann et al. [10] demonstrated that ROT provided consistent results with those obtained by the whole-cell patch-clamp method that enables charge-pulse experiments in transmembrane configuration.

Dielectric spectroscopy (DS) is a well established technique to study the polarization of materials, and its application to biological cells has a long history [11, 12]. DS measures the complex permittivity of a cell suspension over a wide frequency range. Complex relative permittivity $\varepsilon^*$ is defined as $\varepsilon^*=\varepsilon-j\kappa/\omega\varepsilon_0$, where $\varepsilon$ is relative permittivity, $\kappa$ is conductivity (that includes both dc and ac conductivities), $\omega$ is the angular frequency defined as $\omega=2\pi f$, $f$ is the frequency of the applied ac field, $\varepsilon_0$ is the permittivity of vacuum and j is the imaginary unit. In contrast to ROT that is a single-cell technique that reduces theoretical complexity to a large extent, DS dealing with a cell population has drawbacks in theoretical analysis [13]: (1) an appropriate mixture equation and an estimate of the volume fraction of cells in the suspension are required, and (2) broadening of the dielectric spectrum is caused not only by the distributions of cells in size, shape and electric parameters but also by interactions between cells at a high cell concentration. Despite the drawbacks, DS has the following advantages over ROT: (1) measurement is easy and rapid, (2) average dielectric properties of many cells are obtained by a single measurement, (3) perturbation of the cell membrane is small because the applied electric field strength is much lower than

ROT and (4) DS is applicable to small cells and lipid vesicles measuring sub-micrometer in diameter.

To my knowledge, however, DS has never been used for studying the LF dispersion of cells and lipid vesicles treated with lipophilic ions. This is because measurement at low frequencies is seriously blocked by the electrode polarization (EP) effect due to large capacitive impedance at electrode surfaces adjacent to an electrolyte solution [12]. In a previous paper [14], a measurement cell has been devised to reduce the EP effect and to extend the available low-frequency limit one decade. It enabled measurement of the LF dispersion of erythrocyte ghosts [15], being used in this study. The purpose of this paper, therefore, is to demonstrate that DS is applicable to the investigation of the LF dispersion due to translocation of lipophilic ions in the membranes and also to establish the analysis of the LF dispersion to estimate the kinetic parameters of the ion translocation.

## 2. Theoretical considerations

Dielectric properties of biological cells are represented using the single-shell model that is a spherical core (that corresponds to the cytoplasm) is covered with a shell (to the plasma membrane) [16, 17]. Although ordinary cells include intracellular organelles in the cytoplasm, for the sake of simplicity, the model assumes that the cytoplasm has isotropic and homogenous complex relative permittivity $\varepsilon_i^*$ ($\varepsilon_i^*=\varepsilon_i - j\kappa_i/\omega\varepsilon_0$, $\varepsilon_i$ and $\kappa_i$ are the relative permittivity and conductivity of the cytoplasm, respectively). The effective complex relative permittivity $\varepsilon_p^*$ of the shell-sphere including the cytoplasm and the membrane of $\varepsilon_m^*$ ($\varepsilon_m^*=\varepsilon_m - j\kappa_m/\omega\varepsilon_0$, $\varepsilon_m$ and $\kappa_m$ are the relative permittivity and conductivity of the membrane, respectively) can be obtained [17]:

$$\varepsilon_p^* = \varepsilon_m^* \frac{2\varepsilon_m^* + \varepsilon_i^* - 2v\left(\varepsilon_m^* - \varepsilon_i^*\right)}{2\varepsilon_m^* + \varepsilon_i^* + v\left(\varepsilon_m^* - \varepsilon_i^*\right)} \tag{1}$$

with $v=(1-d/R_c)^3$, $d$ is the membrane thickness and $R_c$ is the cell radius.

In the model, the membrane is assumed to have homogeneous and frequency-independent $\varepsilon_m$ and $\kappa_m$. It may be helpful to provide comments for the assumption. In reality, the membrane is not homogeneous and has a hydrophobic layer sandwiched by hydrophilic layers. The electric double layers are formed outside the charged membrane. Furthermore, the relative permittivity near the charged membrane is considered to be lower than bulk water because of the orientation of water molecules [18]. The effects of the hydrophilic layer and the electric double layer on the effective

membrane capacitance $C_m$ defined by $C_m=\varepsilon_m\varepsilon_0/d$ were studied with planar BLMs. The presence of the hydrophilic layers caused a small (2-3%) dispersion of $C_m$ at low frequencies (0.1-100 Hz), which was predicted from the Maxwell-Wagner effect [19]. The effects of the electric double layer on $C_m$ were studied theoretically [20] and experimentally [21], suggesting that $C_m$ is little influenced by the capacitance of the electric double layer for surface charge densities encountered in practice. Although the effect of the low permittivity layers near the charged membrane on $C_m$ is not known, it could be included in the effect of the hydrophilic layer. These results suggest that the membrane can be represented as a homogenous phase of frequency-independent $\varepsilon_m$ and $\kappa_m$, and that the value of $C_m$ is little influenced by the hydrophilic layers and the electrical double layers.

When the cells are suspended in the medium of $\varepsilon_a^*$ ($\varepsilon_a^*=\varepsilon_a - j\kappa_a/\omega\varepsilon_0$, $\varepsilon_a$ and $\kappa_a$ are the relative permittivity and conductivity of the medium, respectively), the effective complex relative permittivity $\varepsilon^*$ of the suspension is obtained by substituting Eq. (1) into the Wagner equation [17]:

$$\varepsilon^* = \varepsilon_a^* \frac{2\varepsilon_a^* + \varepsilon_p^* - 2P\left(\varepsilon_a^* - \varepsilon_p^*\right)}{2\varepsilon_a^* + \varepsilon_p^* + P\left(\varepsilon_a^* - \varepsilon_P^*\right)}, \tag{2}$$

where $P$ is the volume fraction of cells in the suspension. For biological cells that meet the conditions that $d/R_c<<1$, $\kappa_m<<\kappa_i$, and $\kappa_m<<\kappa_a$, Eq. (2) is approximated [17]:

$$\varepsilon^* \approx \varepsilon_h + \frac{\Delta\varepsilon}{1+j\omega\tau_0} + \frac{\kappa_l}{j\omega\varepsilon_0}, \tag{3}$$

where $\varepsilon_h$ is the HF limit of relative permittivity, $\Delta\varepsilon$ is the intensity of the dielectric relaxation (or the difference between the LF and HF limits of relative permittivity in the corresponding dielectric relaxation process), $\tau_0$ is the relaxation time and $\kappa_l$ is the LF limit of conductivity (or the dc conductivity). The dielectric parameters $\varepsilon_h$, $\Delta\varepsilon$, $\tau_0$ and $\kappa_l$ are given in Appendix A.

When the membrane is doped with lipophilic ions, their translocation across the membrane induced by ac electric fields results in dielectric dispersion in the normal component $\varepsilon_{mn}^*$ of the membrane complex relative permittivity. The ions may also move in the plane of the membrane, thereby increasing the tangential component $\kappa_{mt}$ of the membrane conductivity. Sukhorukov et al. [22] assessed these effects on the ROT

spectra of cells doped with lipophilic ions using the single-shell model whose shell has anisotropic and dispersive properties. The assessment suggested that the ROT spectra were little influenced by $\kappa_{mt}$ and were the same as those of the single-shell model having an isotropic and dispersive shell, unless $\kappa_{mt}$ exceeds 0.1 S/m, which value is much higher than that expected from the concentration and the mobility of the adsorbed lipophilic ions. The results provided a valid reason for use of the single shell model with the isotropic and dispersive shell in the analysis of the ROT spectra of cells treated with lipophilic ions [8-10]. In this study, therefore, I adopted the same model and assumed that the membrane has a single relaxation process of intensity $\Delta\varepsilon_m$ and relaxation time $\tau_d$:

$$\varepsilon_m^* = \varepsilon_{mh} + \frac{\Delta\varepsilon_m}{1+j\omega\tau_d} + \frac{\kappa_{ml}}{j\omega\varepsilon_0}, \tag{4}$$

where $\varepsilon_{mh}$ is the HF limit of the membrane relative permittivity and $\kappa_{ml}$ is the LF limit of the membrane conductivity. When $\tau_d$ is much larger than the $\tau_0$ in Eq. (3), the $\varepsilon^*$ of the cell suspension shows LF dispersion (due to the mobile ions in the membrane) apart from the HF dispersion as described in Appendix B.

$$\varepsilon^* \approx \varepsilon_h + \frac{\Delta\varepsilon_H}{1+j\omega\tau_H} + \frac{\Delta\varepsilon_L}{1+j\omega\tau_L} + \frac{\kappa_l}{j\omega\varepsilon_0}, \tag{5}$$

where $\varepsilon_h$ and $\kappa_l$ are the same as in Eq. (3), $\Delta\varepsilon_H$ and $\tau_H$ are the intensity and the relaxation time of the LH dispersion, respectively, and $\Delta\varepsilon_L$ and $\tau_L$ are those of the LF dispersion. The characteristic (or center) frequencies $f_H$ and $f_L$ of the HF and LF dispersions are given by $f_H = 1/(2\pi\tau_H)$ and $f_L = 1/(2\pi\tau_L)$. For biological cells that hold for $\kappa_m << \kappa_a$ and $d << R_c$, the dielectric relaxation parameters $\Delta\varepsilon_H$, $\tau_H$, $\Delta\varepsilon_L$, and $\tau_L$ in Eq. (5) are approximated as

$$\Delta\varepsilon_H \approx \frac{9P}{(2+P)^2}\frac{\varepsilon_{mh}R_c}{d}, \tag{6}$$

$$\tau_H \approx \left(\frac{1}{\kappa_i} + \frac{1-P}{2+P}\frac{1}{\kappa_a}\right)\frac{\varepsilon_{mh}\varepsilon_0 R_c}{d}, \tag{7}$$

$$\Delta\varepsilon_L \approx \frac{9P}{(2+P)^2}\frac{\Delta\varepsilon_m R_c}{d}, \tag{8}$$

$$\tau_L \approx \frac{(1-P)(2+P)}{9P\kappa_a}(\Delta\varepsilon_H + \Delta\varepsilon_L)\varepsilon_0 + \tau_d . \tag{9}$$

To assess the available ranges of $\Delta\varepsilon_m$ and $\kappa_a$ for Eqs. (6), (8) and (9), the values of $\Delta\varepsilon_H$, $\Delta\varepsilon_L$ and $f_L$ calculated from Eqs. (6), (8) and (9) were compared with those estimated from the general equations, Eqs. (1), (2) and (4). The parameter values used in the calculation are relevant to biological cell suspensions: $\varepsilon_a$=80, $\kappa_i$=0.25 S/m, $\varepsilon_i$=60, $\varepsilon_{mh}$=5, $\kappa_{ml}$=0 S/m, $R_c$=5 μm, $d$=5 nm, $P$=0.1 and $f_d$=1 kHz ($f_d$ is the characteristic frequency defined as $f_d=1/(2\pi\tau_d)$). Figure 1 shows the dielectric spectra calculated from the general equations by varying $\Delta\varepsilon_m$ for the case of $\kappa_a$=0.05 S/m. The spectra showed two relaxation processes, which were represented by Eq. (5). The relaxation parameters $\Delta\varepsilon_H$, $\Delta\varepsilon_L$ and $f_L$ obtained by fitting Eq. (5) to the spectra are plotted against $\Delta\varepsilon_m$ in Fig. 2. The value of $\Delta\varepsilon_H$ was independent of $\Delta\varepsilon_m$, and the value of $\Delta\varepsilon_L$ was directly proportional to $\Delta\varepsilon_m$. These relationships were correctly described by Eqs. (6) and (8). The value of $f_L$ slightly decreased with increasing $\Delta\varepsilon_m$, which was represented by Eq. (9) up to $\Delta\varepsilon_m$=50, within an error of 1 %.

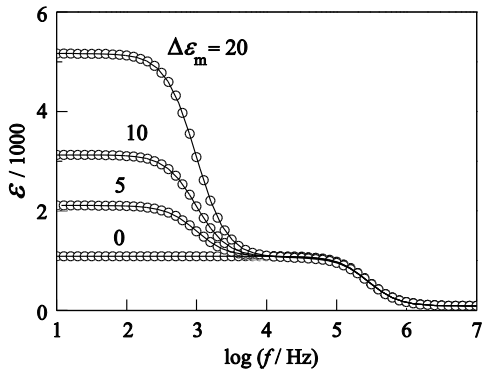


**Fig. 1** Frequency $f$ dependence of the relative permittivity $\varepsilon$ calculated from Eqs. (1), (2) and (4) with $\kappa_a$=0.05 S/m. The intensity $\Delta\varepsilon_m$ of the membrane relaxation is varied as indicated beside each curve. The solid lines are the best-fit curves calculated from Eq. (5).

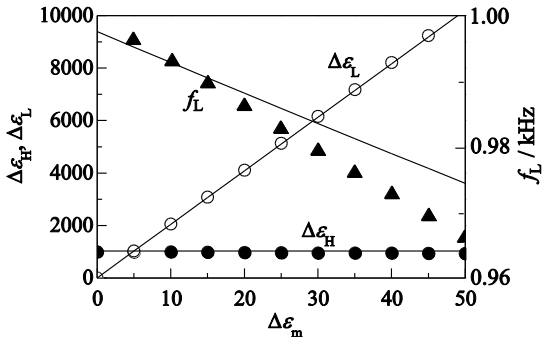


**Fig. 2** The dielectric relaxation parameters $\Delta\varepsilon_H$, $\Delta\varepsilon_L$ and $f_L$ as a function of $\Delta\varepsilon_m$. The data points (●) for $\Delta\varepsilon_H$, (○) for $\Delta\varepsilon_L$ and (▲) for $f_L$ were obtained by fitting Eq. (5) to the dielectric spectra calculated from Eqs. (1), (2) and (4) for $\kappa_a$=0.05 S/m. The solid lines for $\Delta\varepsilon_H$, $\Delta\varepsilon_L$ and $f_L$ were calculated from Eqs. (6), (8) and (9), respectively. The parameter values used are the same as in Fig. 1.

Figure 3 shows the $\kappa_a$-dependence of $\Delta\varepsilon_L$, $\Delta\varepsilon_H$, $\varepsilon_l$ and $f_L$ for the case of $\Delta\varepsilon_m$=10. The values of $\Delta\varepsilon_L$ and $\Delta\varepsilon_H$ calculated from Eqs. (6) and (8) deviated from those obtained from the general equations at $\kappa_a$<0.01 S/m. This is because the assumption of $\tau_d >> \tau_0$ fails at such a low $\kappa_a$. In contrast to $\Delta\varepsilon_L$ and $\Delta\varepsilon_H$, $\varepsilon_l$ ($\varepsilon_l = \Delta\varepsilon_H + \Delta\varepsilon_L$) was not influenced by $\kappa_a$. The value of $f_L$ was equal to that of $f_d$ at $\kappa_a \geq 0.05$ S/m within an error of 1% and decreased with decreasing $\kappa_a$, which tendency was represented by Eq. (9).

In conclusion, Eqs. (6), (8) and (9) can be safely used for analysis of the dielectric spectra at $\kappa_a \geq 0.02$ S/m, and $f_L$ is considered to be equal to $f_d$ at $\kappa_a \geq 0.05$ S/m.

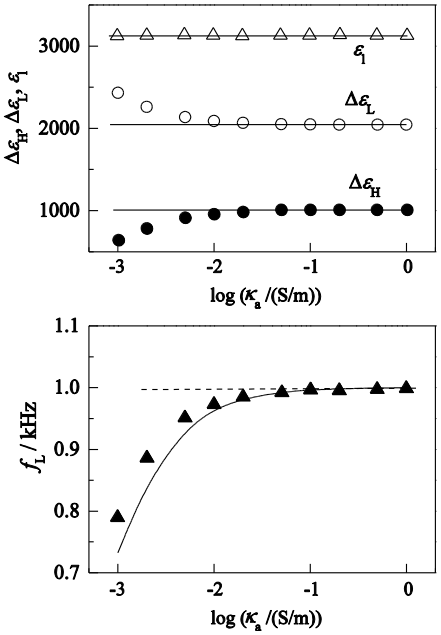

**Fig. 3** The dielectric relaxation parameters $\Delta\varepsilon_H$, $\Delta\varepsilon_L$ , $\varepsilon_i$ and $f_L$ as a function of $\kappa_a$. The data points (●) for $\Delta\varepsilon_H$, (○) for $\Delta\varepsilon_L$, (Δ) for $\varepsilon_i$ and (▲) for $f_L$ were obtained by fitting Eq. (5) to the dielectric spectra calculated from Eqs. (1), (2) and (4). The solid lines for $\Delta\varepsilon_H$, $\Delta\varepsilon_L$ and $f_L$ were calculated from Eqs. (6), (8) and (9), respectively. The solid line for $\varepsilon_i$ was calculated from Eq. (B10) in Appendix B. The dashed line in the plots of $f_L$ indicates the value of $f_d$. The calculation was made for $\Delta\varepsilon_m$=10, and the other parameter values are the same as in Fig. 1.

## 3. Materials and Methods

### *3.1 Preparation of horse erythrocytes*

Erythrocytes were obtained from preserved horse blood purchased from Nippon Biotest Lab. (Tokyo, Japan). Suspensions containing DPA-treated erythrocytes at the same cell concentration were prepared as follows. A given volume (say 0.6 ml) of the blood specimen was transferred into a centrifuge tube and the plasma was removed by centrifugation at 300×g for 5 min, and the collected erythrocytes were washed twice with a medium containing 5 mM Na-phosphate (NaP) buffer (pH 7.2) and 150 mM mannitol (medium A). The erythrocytes were suspended in medium A (10 ml) containing 0-100 μM DPA and incubated at 25 ºC for 10 min. The DPA-doped cells were collected by centrifugation and were resuspended by adding a small volume of the supernatant to attain a given total volume (0.3 ml). In medium A that has one-half of the physiological osmolarity, erythrocytes swelled to change their shape from discoidal to spherical. The cell shape was confirmed by optical microscopy and the mean radius was 2.5 μm.

### *3.2 Cell culture of L5178Y cells*

The strain of murine lymphoblast (L5178Y) was obtained from Health Science Research Resources Bank (Osaka, Japan). Cells were cultured in Fisher's medium supplemented with 10 % horse serum at 37 ºC. Cells collected by centrifugation at 300×g for 5 min were washed with a medium containing 5 mM NaP and 300 mM mannitol twice and then resuspended with the same medium at a volume fraction of 0.1-0.2.

### *3.3 Preparation of unilamellar lipid vesicles*

Large unilamellar vesicles (LUVs) were prepared from Egg phosphatidylcholine (PC) by the extrusion method [23]. 33 μmol Egg PC was dispersed in 1 ml of 5 mM NaP containing 150 mM sucrose. The lipid suspension was subjected to 10 freeze-thawing cycles and followed by 20 times extrusion through a 1 μm pore size polycarbonate

membrane using a LiposoFast device (Avestin, Ottawa, Canada). The suspension was diluted with a medium of 5 mM NaP (7.2) and 150 mM mannitol (medium A) and then was centrifuged at 8000×g for 15 min. The collected LUVs were suspended in medium A containing DPA. After 10 min incubation, the LUV suspension was concentrated by centrifugation to be subjected to DS measurement.

*3.4 Dielectric spectroscopy*

The measurement cell that was developed to reduce the EP effect previously [14] was used in this study. Since the measurement cell leads an error at high frequencies above 100 kHz, a conventional one described previously [24] was also used for correcting the error.

Dielectric measurement has been carried out over a frequency range of 10 Hz to 10 MHz using a 4192A impedance analyzer (Agilent Technologies, Palo Alto, CA). One of the measurement cells was connected to the impedance analyzer using a 16092A Spring Clip Fixture (Agilent Technologies), and the capacitance $C(f)$ and conductance $G(f)$ in the parallel circuit mode were measured as a function of frequency $f$. The measured $C(f)$ and $G(f)$ were converted to the relative permittivity $\varepsilon(f)$ and the conductivity $\kappa(f)$ as $\varepsilon(f)=(C(f)-C_0)/C_1$ and $\kappa(f)=G(f)/(C_1/\varepsilon_0)$ with the dielectric cell constant $C_1$ and the stray capacitance $C_0$ determined for the measurement cell.

## 4. Results

*4.1 Horse erythrocytes*

Figure 4 shows typical dielectric spectra of suspensions of spherical erythrocytes untreated and treated with 1-10 μM DPA. The spherical erythrocytes were prepared by suspending horse erythrocytes in a hypotonic medium containing 5 mM NaP and 150 mM mannitol. Use of the spherical erythrocytes has merit to eliminate the theoretical complexity resulting from the cell shape effects [25, 26]. The dielectric spectra were obtained at the same cell concentration. Since there was little difference in cell size among cells at different DPA concentrations, the suspensions were considered to have the same volume fraction of cells. Two dielectric relaxation processes were clearly seen for DPA-doped erythrocytes, apart from the electrode polarization (EP) effect below 1 kHz. The HF dispersion around 1 MHz was little influenced by DPA, whereas the LF dispersion around 2-3 kHz depended on DPA concentration. Untreated erythrocytes did not show the LF dispersion down to at least 1 kHz, as described in a previous paper [15].

The dielectric spectra of the cell suspensions are subject to broadening due to either

distributions of cells in size, shape and electric parameters or interactions between cells, and furthermore include the EP effect. Hence, instead of Eq. (5), the dielectric spectra were expressed by an empirical equation [15]:

$$\varepsilon^* = \varepsilon_h + \frac{\Delta\varepsilon_H}{1+(j\omega\tau_H)^{\beta_H}} + \frac{\Delta\varepsilon_L}{1+(j\omega\tau_L)^{\beta_L}} + \frac{\kappa_l}{j\omega\varepsilon_0} + A\omega^{-m}, \tag{10}$$

which contains two Cole-Cole relaxation terms (subscripts H and L refer to the HF and the LF dispersion, respectively) and an EP term that is approximately given by $A\omega^{-m}$ with constants $A$ and $m$ [15]. $\Delta\varepsilon$, $\tau$ and $\beta$ are the intensity, the relaxation time and the broadening factor of the Cole-Cole relaxation, respectively. The parameters $\varepsilon_h$, $\Delta\varepsilon_L$, $\tau_L$, $\beta_L$, $\Delta\varepsilon_H$, $\tau_H$, $\beta_H$, $A$, and $m$ in Eq. (10) except the LF limit of the conductivity $\kappa_l$ were determined by the non-linear least squares method to minimize the residual $\chi^2$

$$\chi^2 = \sum\left\{\log\mathrm{Re}\left[\varepsilon^*_{ob}(\omega_i)\right] - \log\mathrm{Re}\left[\varepsilon^*_{th}(\omega_i)\right]\right\}^2, \tag{11}$$

where $\mathrm{Re}[\varepsilon^*_{ob}(\omega_i)]$ and $\mathrm{Re}[\varepsilon^*_{th}(\omega_i)]$ are the real parts of the observed and theoretical complex relative permittivities, respectively.

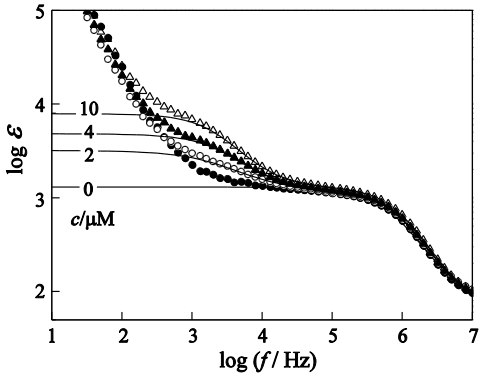


**Fig. 4** Frequency $f$ dependence of the relative permittivity $\varepsilon$ of suspensions of horse erythrocytes treated with 0-10 μM DPA. Data were obtained at the same cell concentration. The solid lines are the best-fit curves calculated from Eq. (10), excluding the EP effect.

The obtained values of $\Delta\varepsilon_L$ and $\Delta\varepsilon_H$ are plotted as a function of DPA concentration $c$ in Fig. 5. The value of $\Delta\varepsilon_H$ was independent of $c$, being the same as that in the absence of DPA. The value of $\Delta\varepsilon_L$ increased with $c$ and tended to level off above 30 μM. The saturation behavior of $\Delta\varepsilon_L$, which has not been reported in previous ROT studies, could

be due to the limited number of DPA ion-binding sites at the membrane interfaces [1] and/or the electrostatic boundary potentials produced within the membrane by the adsorbed DPA ions [5]. Figure 6 shows the characteristic frequencies $f_L$ and $f_H$ plotted against $c$. The value of $f_H$ was independent of $c$, and the value of $f_L$ was almost independent of $c$ except a slight decrease above 30 μM. The results suggest that DPA does not influence the HF dispersion, and that $f_L$ is independent of $c$ below at least 20 μM.

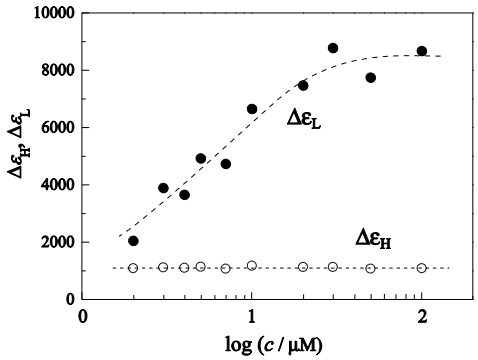


**Fig. 5** The intensity $\Delta\varepsilon_L$ (●) of LF dispersion and the intensity $\Delta\varepsilon_H$ (○) of HF dispersion as a function of DPA concentration $c$. The dashed lines are drawn as a guide to the eye.

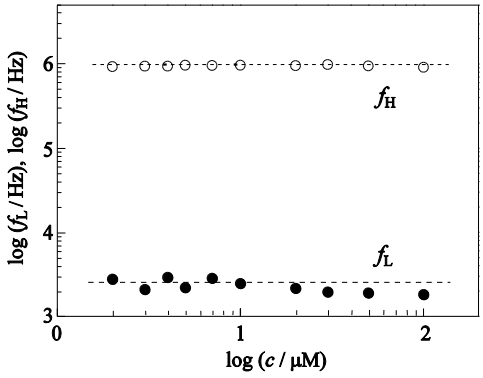


**Fig. 6** The characteristic frequency $f_L$ of LF dispersion and the characteristic frequency $f_H$ of HF dispersion as a function of DPA concentration $c$. The dashed lines are drawn as a guide to the eye.

*4.2 Cultured cells and lipid vesicles*

DPA-doped L5178Y cells were measured in a medium containing 5 mM NaP and 300 mM mannitol, of which conductivity was similar to that used for erythrocytes. Figure 7 shows the dielectric spectrum of the suspension of L5178Y cells treated with 10 μM DPA. Two relaxation processes were found similarly to DPA-doped erythrocytes; the spectrum was well represented by Eq. (10). The LF dispersion of $f_L$=5.2 kHz was clearly

separated from the HF dispersion.

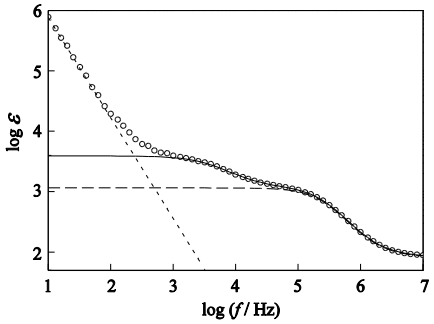


**Fig. 7** Frequency $f$ dependence of the relative permittivity $\varepsilon$ of the suspension of L5178Y cells treated with 10 μM DPA. The solid line is the best-fit curve calculated from Eq. (10) without the EP effect that is indicated by the dotted line. The broken line indicates the HF dispersion.

The large unilameller lipid vesicles (LUVs) of egg PC were prepared by an extruder with polycarbonate membrane filter of a mean pore diameter of 1 μm. The vesicle diameter was 0.6-1 μm, the accurate value being difficult to determine under an optical microscopy. The internal phase of the vesicles contains 5 mM NaP and 150 mM sucrose and the external medium has 5 mM NaP and 150 mM mannitol. Figure 8 shows the dielectric spectra of the LUV suspensions treated with and without DPA. The LUV suspension showed one relaxation process in the absence of DPA as reported previously [27]. In the presence of DPA, however, the LUV suspension showed LF dispersion of $f_L$=4.5 kHz in a similar manner to erythrocytes and L5178Y cells.

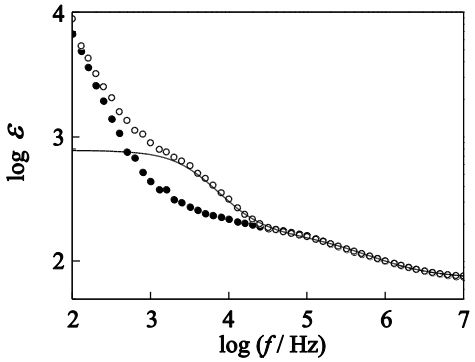


**Fig. 8** Frequency $f$ dependence of the relative permittivity $\varepsilon$ of a LUV suspension in the presence of 10 μM DPA (○) and in the absence of DPA (●). The solid line is the best-fit curves calculated from Eq. (10), excluding the EP effect.

*4.3 Analysis based on mobile charge model*

Following the mobile charge model [1], the dielectric relaxation parameters of the membrane are related to the kinetic parameters of mobile ions, i.e., translocation rate constant $k_i$ in the membrane and area-specific concentration $N_t$ at the membrane interfaces. Since the translocation of ions between the membrane interfaces is much faster than between the membrane interface and the aqueous medium, one can obtain $k_i$ and $N_t$ [1]:

$$\tau_d = \frac{1}{2k_i}, \tag{12}$$

$$\Delta\varepsilon_m = \frac{N_t F^2 d}{2RT\varepsilon_0}, \tag{13}$$

where $F$ is the Faraday constant and $R$ is the gas constant. As described in Section 2, $\tau_d$ is equal to $\tau_L$ for the present experimental conditions, and thus $k_i$ is estimated from $\tau_L$. Using the relation of $\Delta\varepsilon_L/\Delta\varepsilon_H = \Delta\varepsilon_m/\varepsilon_{mh}$ that is obtained from Eqs. (6) and (8), the value of $N_t$ is estimated from

$$N_t = \frac{\Delta\varepsilon_L}{\Delta\varepsilon_H}\frac{2RT\varepsilon_{mh}\varepsilon_0}{F^2 d} = \frac{\Delta\varepsilon_L}{\Delta\varepsilon_H}\frac{2RTC_m}{F^2}, \tag{14}$$

where $C_m=\varepsilon_{mh}\varepsilon_0/d$. In this analysis, only the values of $\tau_L$, $\Delta\varepsilon_L/\Delta\varepsilon_H$ and $C_m$ are required, but it is unnecessary to determine the volume fraction of cells. The values of $C_m$ are available from the literatures, i.e., 10 mF/m$^2$ for L5178Y cells [28] and 7 mF/m$^2$ for erythrocytes [29-31]. Figure 9 shows the values of $k_i$ and $N_t$ estimated for horse erythrocytes of spherical shape and L5178Y cells as a function of the DPA concentration, together with those so far obtained by ROT with human erythrocytes and cultured cells. The values of $k_i$ and $N_t$ were similar to those obtained by ROT, irrespective of different measurement conditions between DS and ROT, i.e., ROT is carried out in lower conductive media and in relatively higher electric field strength than DS.

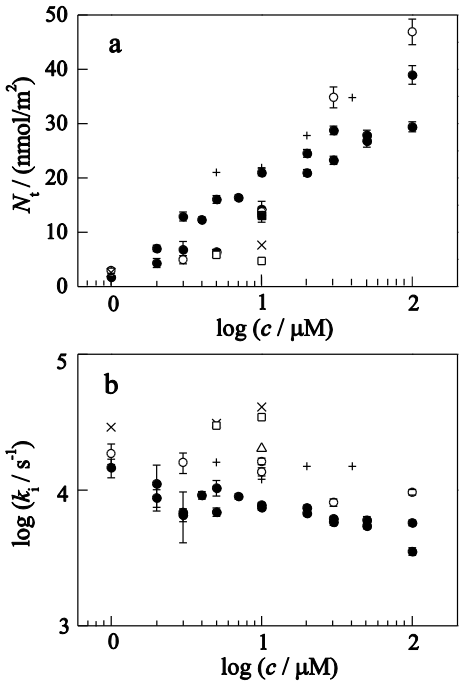


**Fig. 9** (a) Area-specific concentration $N_t$ and (b) translocation rate constant $k_i$ of DPA ions in the membranes of spherical horse erythrocytes (●) and L5178Y (○) are plotted against DPA concentration $c$. The values of $N_t$ and $k_i$ estimated in previous ROT studies are also plotted: human erythrocytes of biconcave shape (×) [8], BH SP2 (+) [9], Jurkat (□) [10] and HEK293 (Δ) [10].

## 5. Discussion

*5.1. Application of DS to dielectric dispersion due to translocation of DPA ions*

This study demonstrated that DS is applicable to the investigation of the dielectric dispersion due to translocation of DPA ions in the membrane. DPA-doped cell suspensions showed LF dielectric dispersion, which was analyzed on the basis of the mobile charge model to provide the kinetic parameters of DPA ions, i.e., the translocation rate constant and the area-specific concentration. The estimated kinetic parameters were comparable to those from previous ROT studies.

DS deals with a population of cells, and, therefore, has drawbacks that do not exist in ROT, i.e., analysis of the dielectric spectrum requires an appropriate mixture equation and an estimate of the volume fraction of cells in the suspension. As for estimation of the kinetic parameters from the LF dispersion, however, any information on the volume fraction is not required. On the other hand, DS capable of rapid and automated measurements makes it possible to monitor time-dependent membrane phenomena using lipophilic ions as a membrane probe.

The LF dispersion was found for LUVs as well as cells. This means that the

interactions of lipophilic ions with lipid molecules can be studied in detail with well-defined lipid membranes. Since, in contrast to planar BLMs that are formed from limited lipids, various natural and synthetic lipids are available for LUVs, use of LUVs will facilitate the quantitative understanding of the interactions. Furthermore, interesting phenomena observed with LUVs such as gel-fluid phase transition and phase separation could be studied through the LF dispersion.

*5.2. Effects of the surface and dipole potential on translocation and binding of DPA ions*

In the mobile charge model, the translocation and binding of lipophilic ions are determined by the potential energy profile in the membrane. The potential energy is the sum of electric terms including the Born-image, surface and dipole potentials and a neutral term [32]. Since the Born-image energy is not so different among cell membranes, we consider the effects of the surface and dipole potentials on the translocation and binding of lipophilic ions.

The surface potential generated by the surface charges spans between the membrane surface and the bulk aqueous solution, being simply represented by the Gouy-Chapman model [33]. The effects of the surface potential were studied with DPA-doped planar BLMs made from negatively charged lipid [2]. The binding of DPA decreased with increasing the ionic strength of the aqueous solution, suggesting that reduction of the negative surface potential facilitates the binding of anionic lipophilic ions at the membrane interfaces.

The dipole potential formed within the membrane originates from the alignment of dipolar residues of the lipids and water molecules at the membrane interfaces [34]. The dipole potential due to the dipolar residues of the lipids is partly cancelled by that of ordered water molecules, but nevertheless positive dipole potential still remains [34]. The positive dipole potential interpreted the large partition coefficient of anionic lipophilic ions compared with cationic ones [32]. It was also found that $k_i$ of DPA in BLMs was strongly influenced by the dipole potential [2]. One of the possible sources for the dipole potential is the ester groups that link the two fatty acid chains to the glycerol backbone. When the ester groups were replaced with the ether groups of a less dipole moment, the value of $k_i$ decreased to a large extent.

*5.3. LF dispersion due to cell membranes of dispersive properties*

Some cell suspensions show LF dispersion below 10 kHz, which is called α-dispersion [12]. The origin of the α-dispersion has not been well understood and it seems unlikely that all the α-dispersions are interpreted by a unique polarization mechanism. The

α-dispersion of bacteria [35, 36] may be due to displacement of counterions around charged cell surfaces, i.e., counterion polarization [37-39]. Erythrocyte ghosts (erythrocytes lysed in hypotonic media) showed α-dispersion which was not found for intact erythrocytes [40]. Lately, it has become apparent that the α-dispersion is interpreted in terms of interfacial polarization by taking into account the presence of a nano-size hole on each ghost [15].

As another candidate for the origin of the α-dispersion, the dielectric dispersion of the membrane itself should be considered, which is possibly evoked by movement of charges and/or reorientation of dipoles in the membranes. Since this type of dispersion has never been reported, DPA-doped cells are a good model to test the possibility that the plasma membrane of dispersive properties contributes to the α-dispersion. This study clearly showed that LF dispersion in the cell suspension is caused by the dielectric dispersion due to translocation of DPA ions in the plasma membrane.

**Appendix A**

*Derivation of Eq. (3) from Eqs. (1) and (2)*

In general, Eq. (1) is rewritten as

$$\varepsilon_p^* = \varepsilon_{ph} + \frac{\Delta\varepsilon_p}{1 + j\omega\tau_p} + \frac{\kappa_{pl}}{j\omega\varepsilon_0}. \tag{A1}$$

This equation indicates that $\varepsilon_p^*$ has a single dielectric relaxation. The relaxation parameters $\varepsilon_{ph}$, $\Delta\varepsilon_p$, $\tau_p$ and $\kappa_p$ are approximated for the case of biological cells that hold for $\kappa_m/\kappa_i << 1$ and $d/R_c << 1$, and Eq. (A1) becomes

$$\varepsilon_p^* \approx \varepsilon_i + \frac{R_c}{d}\left(\frac{\varepsilon_m}{1 + j\omega\tau_p} + \frac{\kappa_m}{j\omega\varepsilon_0}\right). \tag{A2}$$

Combination of Eqs. (A2) and (2) provides

$$\varepsilon^* \approx \varepsilon_h + \frac{\Delta\varepsilon}{1 + j\omega\tau_0} + \frac{\kappa_l}{j\omega\varepsilon_0}. \tag{A3}$$

The dielectric relaxation parameters $\varepsilon_h$, $\Delta\varepsilon$, $\tau_0$ and $\kappa_l$ in Eq. (A3) are obtained [17]:

$$\varepsilon_h = \varepsilon_a \frac{(1+2P)\varepsilon_i + 2(1-P)\varepsilon_a}{(1-P)\varepsilon_i + (2+P)\varepsilon_a}, \tag{A4}$$

$$\Delta\varepsilon = \frac{9P}{(2+P)^2}\frac{\varepsilon_m R_c}{d}, \tag{A5}$$

$$\tau_0 = \left(\frac{1}{\kappa_i} + \frac{1-P}{2+P}\frac{1}{\kappa_a}\right)\frac{\varepsilon_m \varepsilon_0 R_c}{d}, \tag{A6}$$

$$\kappa_l = \kappa_a \frac{2(1-P)}{(2+P)}. \tag{A7}$$

The symbols $\varepsilon_i$, $\varepsilon_a$, $\varepsilon_m$, $\kappa_a$, $d$, $R_c$ and $P$ for the electrical and structural parameters of the single-shell model are the same as those described in section 2.

**Appendix B**

*The intensity and the relaxation time of the LF dispersion*

We consider that the membrane has a relaxation process of a single relaxation time $\tau_d$ that is much larger than $\tau_p$ in Eq. (A1). At low frequencies such that $\omega\tau_p << 1$ the equivalent complex relative permittivity of the cell $\varepsilon_p^*$ given by Eq. (A2) becomes

$$\varepsilon_p^* \approx \frac{R_c}{d}\varepsilon_m^* = \frac{R_c}{d}\left(\varepsilon_{mh} + \frac{\Delta\varepsilon_m}{1+j\omega\tau_d} + \frac{\kappa_m}{j\omega\varepsilon_0}\right), \tag{B1}$$

Substituting Eq. (B1) for $\varepsilon_p^*$ in Eq. (2), we obtain

$$\varepsilon^* = \frac{A + (j\omega)E + (j\omega)^2 B}{C + (j\omega)F + (j\omega)^2 D}\varepsilon_a^* \tag{B2}$$

The variables *A*-*F* are given by Eqs. (B3)-(B8), which are approximated for the case of biological cells that hold for $\kappa_m << \kappa_a$ and $d << R_c$.

$$A = \left[2(1-P)\kappa_a + (1+2P)\frac{R_c}{d}\kappa_m\right]\frac{1}{\varepsilon_0} \approx 2(1-P)\kappa_a\frac{1}{\varepsilon_0} \tag{B3}$$

$$B=\left[2(1-P)\varepsilon_a+(1+2P)\frac{R_c}{d}\varepsilon_{mh}\right]\tau_d\approx(1+2P)\frac{R_c}{d}\varepsilon_{mh}\tau_d \tag{B4}$$

$$C=\left[(2+P)\kappa_a+(1-P)\frac{R_c}{d}\kappa_m\right]\frac{1}{\varepsilon_0}\approx(2+P)\kappa_a\frac{1}{\varepsilon_0} \tag{B5}$$

$$D=\left[(2+P)\varepsilon_a+(1-P)\frac{R_c}{d}\varepsilon_{mh}\right]\tau_d\approx(1-P)\frac{R_c}{d}\varepsilon_{mh}\tau_d \tag{B6}$$

$$\begin{aligned}E&=2(1-P)\varepsilon_a+(1+2P)\frac{R_c}{d}(\varepsilon_{mh}+\Delta\varepsilon_m)+\left[2(1-P)\kappa_a+(1+2P)\frac{R_c}{d}\kappa_m\right]\frac{\tau_d}{\varepsilon_0}\\&\approx(1+2P)\frac{R_c}{d}(\varepsilon_{mh}+\Delta\varepsilon_m)+2(1-P)\kappa_a\frac{\tau_d}{\varepsilon_0}\end{aligned} \tag{B7}$$

$$\begin{aligned}F&=(2+P)\varepsilon_a+(1-P)\frac{R_c}{d}(\varepsilon_{mh}+\Delta\varepsilon_m)+\left[(2+P)\kappa_a+(1-P)\frac{R_c}{d}\kappa_m\right]\frac{\tau_d}{\varepsilon_0}\\&\approx(1-P)\frac{R_c}{d}(\varepsilon_{mh}+\Delta\varepsilon_m)+(2+P)\kappa_a\frac{\tau_d}{\varepsilon_0}\end{aligned} \tag{B8}$$

In general, Eq. (B2) has two relaxation terms. However, the HF relaxation term is meaningless because we confine ourselves to the low frequency region where Eq. (B1) holds. The relaxation time of the LF dispersion is given by

$$\tau_L\approx\frac{F}{C}\approx\frac{(1-P)}{(2+P)\kappa_a}\frac{R_c}{d}(\varepsilon_{mh}+\Delta\varepsilon_m)\varepsilon_0+\tau_d\,. \tag{B9}$$

At $\omega\to0$, neglecting the terms including $(\mathrm{j}\omega)^2$ in Eq. (B2), we can obtain the effective relative permittivity $\varepsilon_l$ as

$$\varepsilon_l=\frac{1}{C^2}\left[\varepsilon_a AC-\frac{\kappa_a}{\varepsilon_0}(AF-CE)\right]=\frac{9PR_c}{(2+P)^2}\frac{\varepsilon_{mh+}\Delta\varepsilon_m}{d}\,. \tag{B10}$$

If the intensity of the high-frequency relaxation $\Delta\varepsilon_{\mathrm{H}}$ is given by Eq. (A5) obtained for the non-dispersive membrane with $\varepsilon_{\mathrm{m}}=\varepsilon_{\mathrm{mh}}$, the intensity $\Delta\varepsilon_{\mathrm{L}}$ of the LF dispersion becomes

$$\Delta\varepsilon_L = \varepsilon_l - \Delta\varepsilon_H = \frac{9PR_c}{(2+P)^2}\frac{\Delta\varepsilon_m}{d}\,. \tag{B11}$$

Using Eq. (B10), Eq. (B9) is rewritten as

$$\tau_L = \frac{(1-P)(2+P)}{9P\kappa_a}\varepsilon_l\varepsilon_0 + \tau_d\,. \tag{B12}$$

**References**

[1] B. Ketterer, B. Neumcke, P. Läuger, Transport mechanism of hydrophobic ions through lipid bilayer membranes, J. Membr. Biol. 5 (1971) 225-245.

[2] R. Benz, P. Läuger, Transport kinetics of dipicrylamine through lipid bilayer membranes. Effects of membrane structure, Biochim. Biophys. Acta 468 (1977) 245-258.

[3] R. Benz, P. Läuger, K. Janko, Transport kinetics of hydrophobic ions in lipid bilayer membranes, charge-pulse relaxation studies, Biochim. Biophys. Acta 455 (1976) 701-720.

[4] R. Benz, Structural requirement for the rapid movement of charged molecules across membranes, Biophys. J. 54 (1988) 25-33.

[5] O. S. Andersen, S. Feldberg, H. Nakadomari, S. Levy and S. McLaughlin, Electrostatic interactions among hydrophobic ions in lipid bilayer membranes, Biophys. J. 21 (1978) 35-70

[6] A. D. Pickar, W. Brown, Capacitance of bilayers in the presence of lipophilic ions, Biochim. Biophys. Acta 733 (1983) 181-185.

[7] R. Benz, F. Conti, Structure of the squid axon membrane as derived from charge-pulse relaxation studies in the presence of adsorbed lipophilic ions, J. Membr. Biol. 59 (1981) 91-104.

[8] V. L. Sukhorukov, U. Zimmermann, Electrorotation of erythrocytes treated with dipicrylamine: Mobile charges within the membrane show their “signature” in rotational spectra, J. Membr. Biol. 153 (1996) 161-169.

[9] M. Kürschner, K. Nielsen, C. Andersen, V. L. Sukhorukov, W. A. Schenk, R. Benz, U. Zimmermann, Interaction of lipophilic ions with the plasma membrane of mammalian cells studied by electrorotation, Biophys J. 74 (1998) 3031-3043.

[10] D. Zimmermann, M. Kiesel, U. Terpitz, A. Zhou, R. Reuss, J. Kraus, W. A. Schenk, E. Bamberg, V. L. Sukhorukov, A combined patch-clamp and electrorotation study of the voltage- and frequency-dependent membrane capacitance caused by structurally dissimilar lipophilic anions, J. Membr. Biol. 221 (2008) 107-121.

[11] K. S. Cole, Membrane, Ion, and Impulses, University of California Press, Berkeley, 1968

[12] H. P. Schwan, Electrical properties of tissue and cell suspensions. in: J. H. Lawrence, C. A. Tobias (Eds.). Advances in Biological and Medical Physics, vol. 5, Academic Press, New York, 1957, pp. 147-209.

[13] J. Gimsa, D. Wachner, A unified resistor-capacitor model for impedance,

dielectrophoresis, electrorotation, and induced transmembrane potential, Biophys. J. 75 (1998) 1107-1116

[14] K. Asami, Design of a measurement cell for low-frequency dielectric spectroscopy of biological cell suspensions, Meas. Sci. Technol. 22 (2011) 085801.

[15] K. Asami, Dielectric spectroscopy reveals nanoholes in erythrocyte ghosts, Soft Matter 8 (2012) 3250-3257.

[16] H. Pauly, H. P. Schwan, Über die Impedanz einer Suspension von kugelförmigen Teilchen mit einer Schale, Z. Naturforsch. 14b (1959) 125-131.

[17] T. Hanai, Electrical properties of emulsions. in: P. Sherman (Ed.), Emulsion Science, Academic Press, London, 1968, pp.353-478

[18] E. Gongadze, A. Iglič, Decrease of permittivity of an electrolyte solution near a charged surface due to saturation and excluded volume effects, Bioelectrochemistry 87 (2012) 199-203.

[19] H. G. L. Coster, J. R. Smith, The molecular organization of bimolecular lipid membranes. A study of the low frequency Maxwell-Wagner impedance dispersion, Biochim. Biophys. Acta 373 (1974) 151-164

[20] C. T. Everitt, D. A. Haydon, Electrical capacitance of a lipid membrane separating two aqueous phases, J. Theoret. Biol. 18 (1968) 371-379

[21] S. White, The surface charge and double layers of thin lipid films formed from neutral lipids, Biochim. Biophys. Acta 323 (1973) 343-350

[22] V. L. Sukhorukov, G. Meedt, M. Kürschner, U. Zimmermann, A single-shell model for biological cells extended to account for the dielectric anisotropy of the plasma membrane, J. Electrostatics 50 (2001) 191-204.

[23] M. J. Hope, M. B. Bally, G. Webb, P. R. Cullis, Production of large unilamellar vesicles by a rapid extrusion procedure. Characterization of size distribution, trapped volume and ability to maintain a membrane potential, Biochim. Biophys. Acta 812 (1985) 55-65.

[24] K. Asami, A. Irimajiri, T. Hanai, N. Shiraishi, K. Utsumi, Dielectric analysis of mitochondria isolated from rat liver. I. Swollen mitoplasts as simulated by a single-shell model, Biochim. Biophys. Acta 778 (1984) 559-569

[25] K. Asami, T. Hanai, N. Koizumi, Dielectric approach to suspensions of ellipsoidal particles covered with a shell in particular reference to biological cells. Japanese J. Appl. Phys. 19 (1980) 359-365

[26] J. Gimsa, A comprehensive approach to electro-rotation, electrodeformation, electrophoresis, and electrorotation of ellipsoidal particles and biological cells,

Bioelectrochemistry 54 (2001) 23-31

[27] A. Di Biasio, C. Cametti, Dielectric properties of aqueous zwitterionic liposome suspensions, Bioelectrochemistry 70 (2002) 328-334.

[28] A. Irimajiri, Y. Doida, T. Hanai, A. Inouye, Passive electrical properties of cultured murine lymphoblast (L5178Y) with reference to its cytoplasmic membrane, nuclear envelope, and intracellular phases, J. Membr. Biol. 38 (1978) 209-232.

[29] S. Takashima, K. Asami, Y. Takahashi, Frequency domain studies of impedance characteristics of biological cells using micropipette technique. I. Erythrocyte, Biophys. J. 54 (1988) 995-1000.

[30] K. Asami, Y. Takahashi, S. Takashima, Dielectric properties of mouse lymphocytes and erythrocytes, Biochim. Biophys. Acta 1010 (1989) 49-55.

[31] A. Di Biasio, C. Cametti, D-glucose-induced alterations in the electrical parameters of human erythrocyte cell membrane, Bioelectrochemistry 77 (2010) 151-157.

[32] R. F. Flewelling, W. L. Hubbell, The membrane dipole potential in a total membrane potential model. Applications to hydrophobic ion interactions with membranes, Biophys. J. 49 (1986) 541-52

[33] S. McLaughlin, The electrostatic properties of membranes, Annu. Rev. Biophys. Biophys. Chem. 18 (1989) 113-36

[34] L. Wang, Measurements and implications of the membrane dipole potential, Annu. Rev. Biochem., 81 (2012) 615-35

[35] C. W. Einolf, E. L. Carstensen, Passive electrical properties of microorganisms. IV. Studies of the protoplasts of *Micrococcus lysodeikticus*, Biophys. J. 9 (1969) 634-643.

[36] C. W. Einolf and E. L. Carstensen, Passive electrical properties of microorganisms. V. Low-frequency dielectric dispersion of bacteria, Biophys. J. 13 (1973) 8-13.

[37] G. Schwarz, A theory of the low-frequency dielectric dispersion of colloidal particles in electrolyte solution, J. Phys. Chem. 66 (1962) 2636-42.

[38] S. S. Dukhin, V. N. Shilov, Dielectric phenomena and the double layer in disperse systems and polyelectrolytes, Kerter Publishing House, Jerusalem, 1974

[39] C. Grosse, A. V. Delgado, Dielectric dispersion in aqueous colloidal systems, Current Opinion in Colloid Interface Sci. 15 (2010) 145-159.

[40] H. P. Schwan, E. L. Carstensen, Dielectric properties of the membrane of lysed erythrocytes, Science 125 (1957) 985-6